16th ICAAR LISBOA 2020-2022

16th International Conference on
Alkali-Aggregate Reaction in Concrete
Lisboa | LNEC | Portugal | 31 May - 2 June 2022

http://icaar2020-2022.lnec.pt

Impact of different added alkalis on concrete expansion due to ASR

Andreas Leemann (1)

(1) Swiss Federal Laboratories for Materials Testing and Research (Empa), Dübendorf, Switzerland, andreas.leemann@empa.ch

Abstract

Accelerated alkali silica reaction (ASR) tests usually incorporate the addition of alkalis to the mixing water or the immersion of test specimens in alkaline solutions. These measures are taken to increase the reaction potential and to compensate for alkali leaching. Mainly NaOH and in a few cases KOH are used for this ASR-enhancing purpose. Lithium on the other hand does not enhance ASR but can be used to supress ASR, if added in sufficient amounts. The effect of rubidium and caesium on expansion is not known. In this study the five mentioned alkalis are added to concrete tested with the concrete prism test to investigate their influence on expansion. The composition of the ASR products formed is determined with scanning electron microscopy and energy-dispersive X-ray spectroscopy. Additionally, the effect of the different alkalis on dissolution kinetics is studied.

The effect of the different alkalis on concrete expansion differs. However, these differences cannot be explained purely based on dissolution kinetics.

***Keywords**: alkali-silica reaction; alkali addition; dissolution kinetics; concrete prism test*

1. INTRODUCTION

The addition of alkalis to the mixing water of mortar and concrete and the use of alkaline soaking solutions are commonly used for accelerated testing in the field of alkali-silica reaction (ASR) [1-5]. Usually, sodium hydroxide (NaOH) is added to boost the alkali level of mortar or concrete [2-5]. The use of potassium hydroxide (KOH) is less widespread for this purpose, [1], although cement clinker usually contains a higher amount of K than Na. On the other hand, alkalis are not only useable to enhance ASR. The addition of lithium (Li) salts to mortar and concrete is able to suppress expansion and avoid damages due to ASR [6-12]. The effect of the other alkalis rubidium (Rb) and caesium (Cs) on ASR is not known. Cs addition has recently been employed as a tracer to follow the ASR sequence down to a sub-micrometre scale [13].

The goal of this study is to determine the effect of the different alkalis on ASR-induced expansion. Li, Na, K, Li and Cs are added to concrete in the form of nitrate in order to study their effect on expansion. Moreover, the microstructure of the concrete and the composition of the ASR products are investigated using scanning electron microscopy (SEM) and energy-dispersive X-ray spectroscopy (EDS). Additional experiments are conducted in order to determine to impact of the different alkalis on SiO_2 dissolution kinetics.

2. MATERIALS AND METHODS

2.1 Materials

A Portland cement (CEM I 42.5 N, see Table 2.1) content of 410 kg/m^3 and a water-to-cement-ratio (w/c) of 0.45 was used for concrete production. The Na_2O-equivalent of the cement was 0.79 kg/m^3 resulting in a total alkali content in the reference concrete (C-Ref) of 3.25 kg/m^3. The aggregate of alluvial origin consisted of gneiss and quartzite. 1790 kg/m^3 of aggregates were added in four different grain size fractions (0/4 mm: 40 mass-%, 4/8 mm: 15 mass-%, 8/16 mm: 20 mass-%, 16/22 mm: 25 mass-%). Alkalis (Li, Na, K, Li and Cs) were added in the form of nitrate. The molar ratio of the added alkali nitrates resulted in a molar ratio of added alkali to alkali present in the cement equal to 0.38. The alkali nitrates were dissolved in the mixing water before concrete production.

Table 2.1: Composition of CEM I 42.5 N and microsilica.

Oxides [mass-%]	SiO_2	Al_2O_3	Fe_2O_3	Cr_2O_3	MnO	TiO_2	P_2O_5	CaO	MgO	K_2O	Na_2O	SO_3	LOI	sum
CEM I 42.5	20.14	4.56	3.25	0.013	0.05	0.368	0.24	63.0	1.9	0.96	0.16	3.25	2.06	99.85
microsilica	93.00	0.94	0.13	n.a.	0.03	0.01	0.05	0.36	0.74	1.09	0.39	0.54	2.67	99.95

Three prisms (70 × 70 × 280 mm^3) were produced with each concrete mixture. The prisms were demoulded after 24h following the protocol of the concrete prism test (CPT) [5].

Samples from one of the prisms per mixture were taken after 8 weeks. They were cut to appropriate size for microscopy, dried in an oven for three days at 50 °C, epoxy impregnated, polished and carbon coated.

Microsilica was used for the dissolution experiments (Table 2.1). The standard alkaline solution contained 0.08 M NaOH and 0.32 M KOH. Alkalis were added again as nitrates in a concentration of 0.13 M/l. 500 ml of the different alkaline solutions including the alkali nitrates were pre-stored in Nalgene bottles at 40 °C. Then 0.5 g of microsilica were added to each of them. 5 ml of solution were sampled after 3h, 1d, 2d, 7d, 14d and 28d and subsequently analysed. First, the experiments were conducted at 60 °C. However, Si concentration reached a level close to silica saturation already after 1d. Therefore, storing temperature of the samples was decreased to 40 °C.

2.2 Methods

The solutions taken from the bottles containing microsilica were diluted by a factor of 10 with HNO_3 (6.5%) to prevent the precipitation of solid phases. The total concentrations of the elements analysed were determined using a Dionex DP ICS-3000 ion chromatograph.

The CPT according to the Swiss standard SIA 262-1 [5] was used. The test requires storage of the prims (70 × 70 × 280 mm^3) at 60 °C and 100 % relative humidity (RH) for 20 weeks with measurements every 4 weeks. The limit value of expansion is 0.20 ‰.

The microstructure of the concrete was analysed with a scanning electron microscope (SEM) FEI Quanta 650 using a pressure between 3.0 and 4.0 × 10^{-6} Torr. Chemical analysis was performed by energy-dispersive X-ray spectroscopy (EDS) with a Thermo Noran Ultra Dry 60 mm^2 detector and Pathfinder X-Ray Microanalysis Software. An acceleration voltage of 12.0 or 12.5 kV was used for imaging and EDS point analysis. Between 200-300 EDS point analyses of ASR products formed in aggregates were conducted per concrete.

3. RESULTS

3.1 Dissolution kinetics

The addition of alkali nitrates has an impact on Si dissolution kinetics. The stable concentrations of the alkalis during the duration of the dissolution experiment clearly indicates that no precipitation occurs (data not shown). After 3h the order of Si dissolution of the mixes with alkali nitrate addition stored at 40 °C is the following: Li < Cs < Rb < Na < K (Figures 3.1 and 3.2). The reference without addition shows about the same Si concentration as the one with KNO_3 addition. Si dissolution after 3h is the same for the solutions stored at 60 °C (data not shown). However, this changes with ongoing dissolution. When Si concentration is close to saturation after 7d for the solutions stored at 40 °C, Si concentration is increasing with decreasing atomic number: Cs < Rb < K < Na< Li. After saturation is reached at 14d, there are only minor differences between Si concentrations in the different solutions.

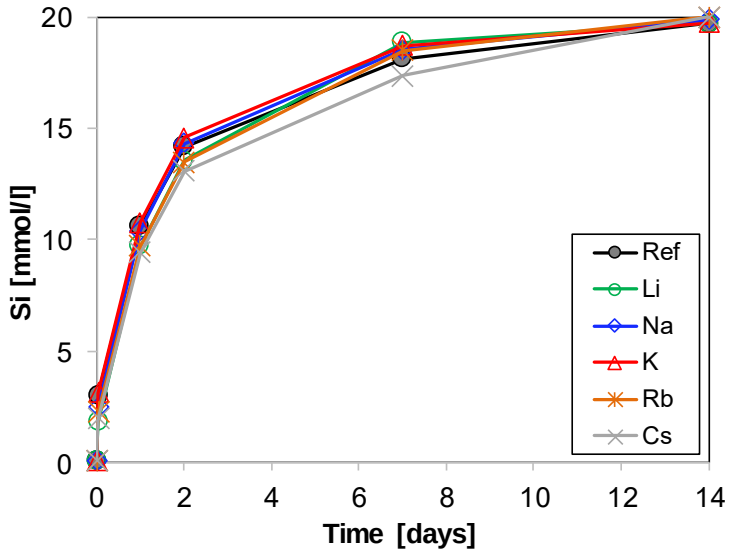

Figure 3.1: Absolute Si concentrations as a function of time in an alkaline solution (0.08 M NaOH and 0.32 M KOH) without addition of nitrates (Ref) and the addition of 0.13 M alkali nitrates.

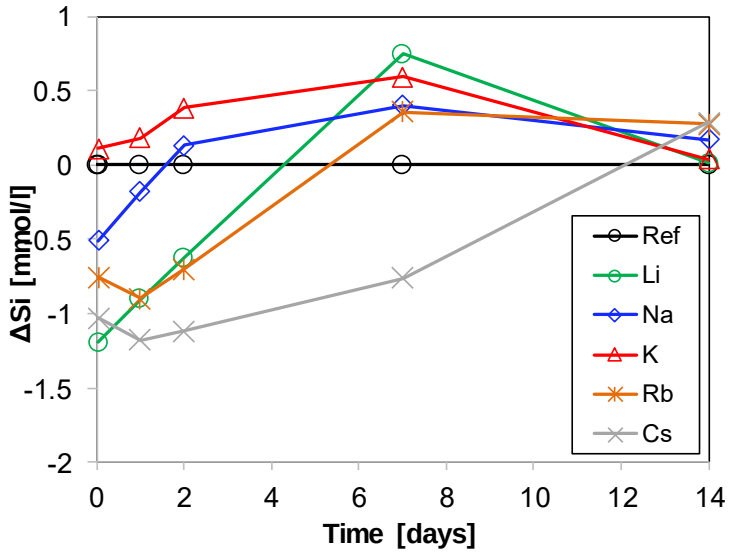

Figure 3.2: Deviations of Si concentrations relative to the reference concentration as a function of time in an alkaline solution (0.08 M NaOH and 0.32 M KOH) without addition of nitrates (Ref) and the addition of 0.13 M alkali nitrates.

3.2 Concrete Expansion

The concrete mixtures show an expansion between 0.42 and 1.24 ‰ after 20 weeks (Figure 3.3). As such, all of them are above the limit value of 0.20 ‰ defined in [5]. Concrete C-Li shows the lowest expansion, slightly more than concrete C-Ref. The expansion increases with the atomic number from concrete C-Li, C-Na C-K to C-Rb reaching the maximum value of 1.24 ‰. Concrete C-Cs does not follow this trend and exhibits a lower expansion of 0.91 ‰ ranking it just below concrete C-Na.

All concrete mixtures display a mass increase during the test (Figure 3.4). The mass increase does not show the same ranking order as expansion, although concrete C-Ref shows the smallest mass increase. The mass of concrete C-Na and C-K increases the most with concrete C-Rb, C-Cs and C-Li showing a lower mass gain.

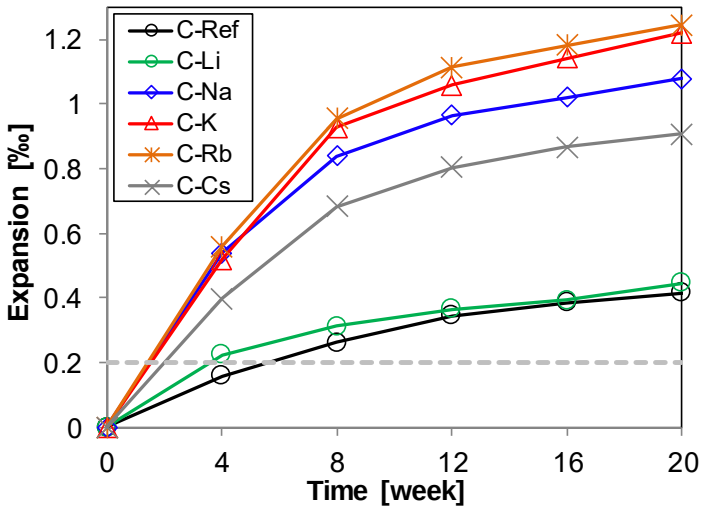

Figure 3.3: Expansion as a function of time of the different concrete mixtures.

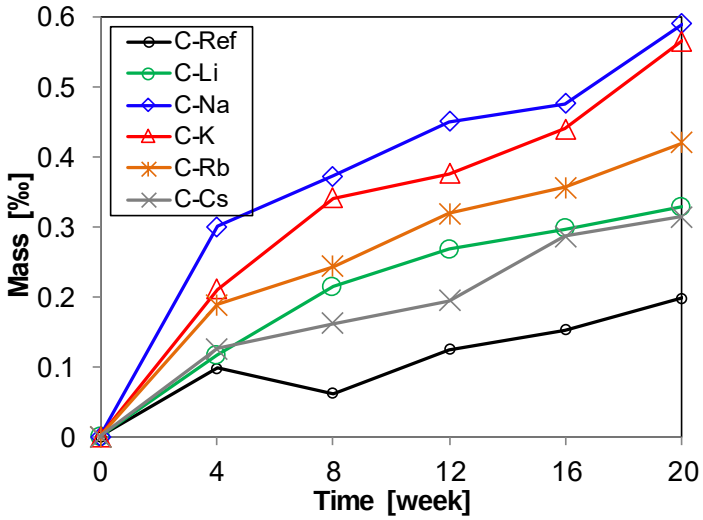

Figure 3.4: Relative mass change as a function of time of the different concrete mixtures.

3.3 Composition of reaction products

The ASR products in the uncracked aggregates are mainly present as thin layers in the micrometre and sub-micrometre scale in pre-existing gaps between adjacent minerals grains. In the case of concrete C-Li, C-Na and C-K these thin layers can only be confirmed by performing an EDS line scan perpendicular to adjacent minerals grains confirming the presence of alkalis and calcium and with them the presence of ASR products. Due to the high atomic number of Rb and in particular Cs, ASR products in concrete C-Rb and C-Cs are easily identified without EDS-analysis by the increased backscattering contrast (Figure 3.5). This allows to follow the formation of ASR products and with it the reaction sequence with a resolution down to a nanometre scale as described in [13]. ASR products start to form in the aggregates close to the interface to the cement paste. Then they progress as an ingressing front towards the interior of the aggregates filling pre-existing porosity, mainly the gaps between adjacent mineral grains. The point of cracking of individual aggregates is not directly linked to the depth the front of ASR products has reached in the aggregates. In some aggregates, the front of ingressing ASR products has reached a maximum depth of a few hundred micrometres at the time of cracking. In other aggregates, ASR products fill all pre-existing porosity of an aggregate without cracks occurring. When aggregates finally crack, there is an extrusion of ASR products into the cement paste resulting in a plug of ASR products at the interface to the cement paste. The extruded ASR products and the plug at the interface to the cement paste are structure-less, while the ASR products starting to fill the cracks after the initial

cracking often display a platelet morphology (Figure 3.6). In [14] it was shown that the structure-less products corresponds to an amorphous phase and the second one to a crystalline one. However, this distinction is not easy to make in some ASR products present in the eight week old concrete, as the size of the platelets are in the nanometre scale. They are considerably larger in decades-old concrete of structures [14].

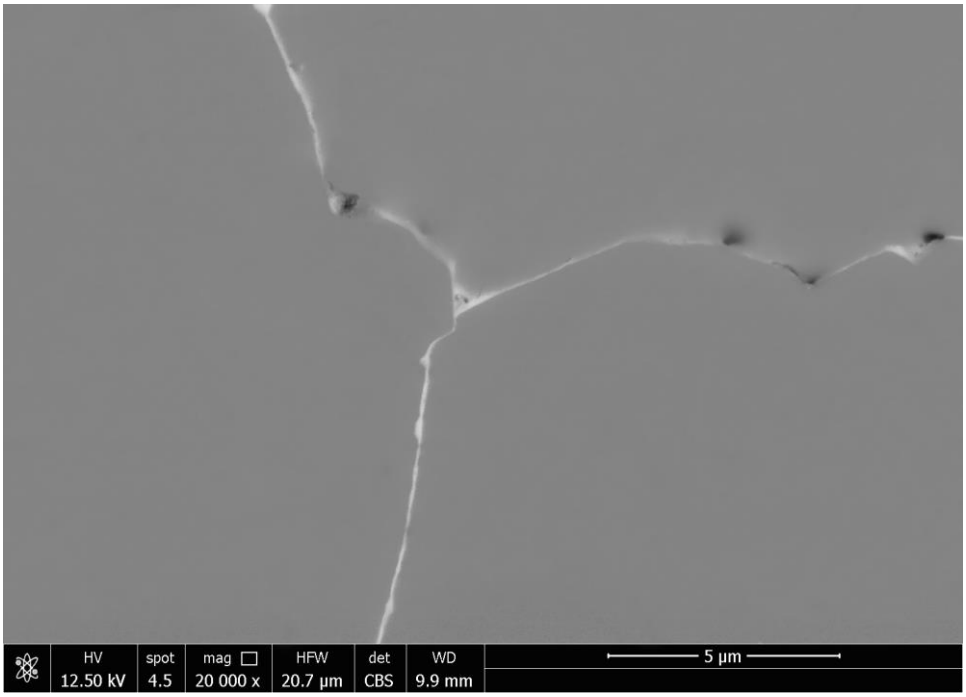

Figure 3.5: Thin layers of ASR products between adjacent quartz grains in an uncracked aggregate of concrete C-Cs. The ASR products stand out due to the increased backscattering contrast caused by the presence of Cs. Horizontal field width (HFW) = 20.7 µm.

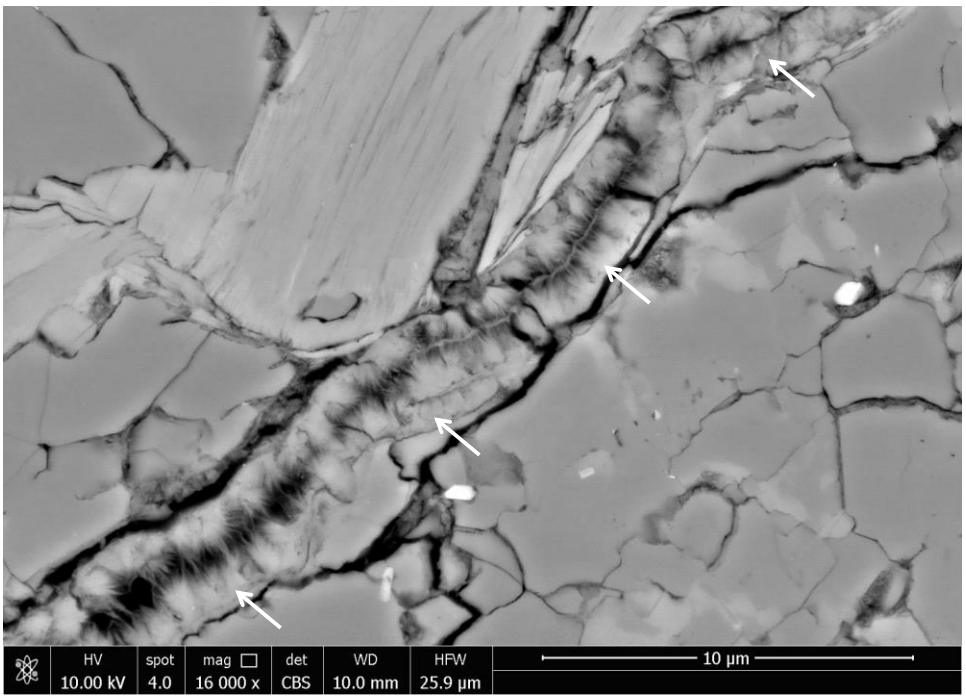

Figure 3.6: ASR products (white arrows) in a crack of a gneiss aggregate in concrete C-K with a platelet morphology. HFW = 25.9 µm.

The composition of the ASR products formed in the aggregates of the different concrete mixture can be shown best using atomic ratio plots. Concrete C-Li shows both the lowest Ca/Si-ratio and the lowest (Na+K)/Si-ratio (Figure 3.7). The highest values of both ratios are displayed by concrete C-K. While Na/K-ratio of concrete C-Na is clearly increased by the $NaNO_3$ addition, concrete C-K shows a value not significantly lower than the other doped concrete mixtures (Figure 3.8). With a value of 0.25 it corresponds exactly to the atomic Na/K ratio present in the cement. Concrete C-Ref exhibits even a slightly lower Na/K-ratio than concrete C-K. Atomic Ca/Si- and Na/K-ratio of concrete C-Rb and C-Cs are both close to the average of the other concrete mixtures.

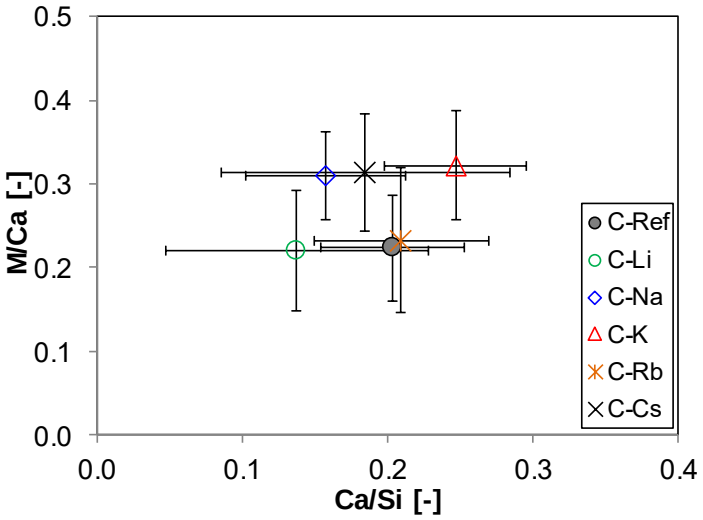

Figure 3.7: Atomic M/Ca-ratio as a function of the atomic Ca/Si-ratio of the ASR products formed in aggregates of the different concrete mixtures. M is used to denominate alkalis.

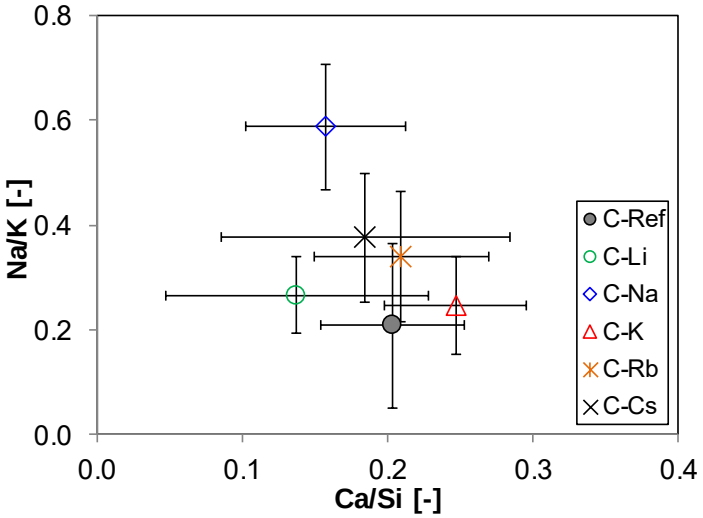

Figure 3.8: Atomic Na/K-ratio as a function of the atomic Ca/Si-ratio of the ASR products formed in aggregates of the different concrete mixtures.

Single EDS point analysis of concrete C-Li, C-Na and C-K are used to show the impact of alkali addition to the composition of the ASR products (Figure 3.9 and 3.10). As it is already evident from the mean values presented in Figures 3.7 and 3.8, alkali addition does influence calcium incorporation of the ASR products. Concrete C-K clearly has a higher Ca/Si ratio in the ASR products than concrete C-Na. Concrete C-Li has by far the highest number of points with a very low Ca/Si-ratio. Na addition results in a high Na/K-ratio in concrete C-Na, while the addition of K lowers the Na/K-ratio of concrete C-K (Figure 3.10).

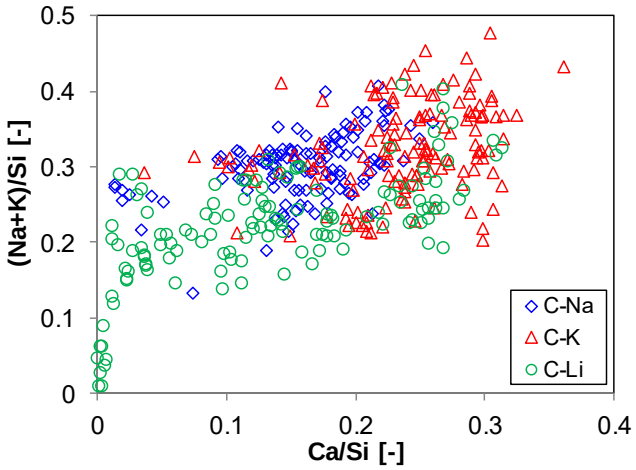

Figure 3.9: Atomic (Na+K)/Si-ratio as a function of the atomic Ca/Si-ratio of the ASR products formed in aggregates of concrete C-Li, C-Na and C-K.

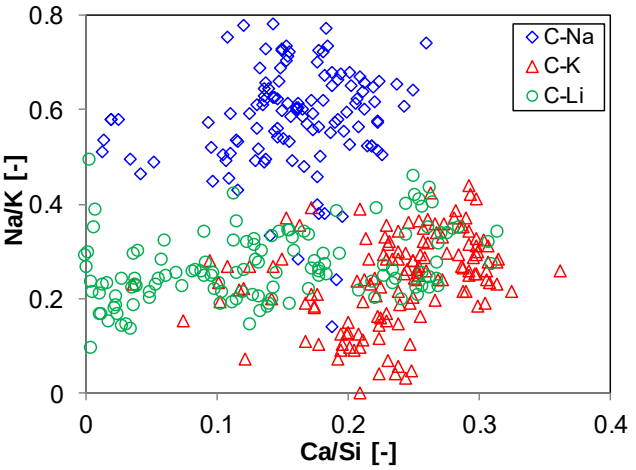

Figure 3.10: Atomic Na/K-ratio as a function of the atomic Ca/Si-ratio of the ASR products formed in aggregates of concrete C-Li, C-Na and C-K.

4. DISCUSSION

4.1 SiO_2 dissolution and concrete expansion

The formation of ASR products is a result of SiO_2 dissolution followed by precipitation. It can be expected that the kinetics of this process govern concrete expansion rate. As the dissolution rates is decisive for the time until supersaturation is reached and ASR products can form, they can be expected to be important for the kinetics of concrete expansion. However, there are little data concerning the impact of different alkalis on this two-step process. Exposed to hydroxide solutions the rate of dissolution has been observed to increase in the order: Li ≈ Cs < Rb ≈ Na < K [15], in agreement with the observations in this study. The alkali nitrates added to the standard alkaline solution (0.08 M NaOH, 0.32 M KOH) affect the dissolution rate at low Si concentrations in the following way: Li < Cs < Rb < Na < Ref ≈ K. These results do not differ much to the referenced ones except that differences between the different alkalis seem to be clearer in this study. However, Si concentration decreases with increasing atomic number of the alkali ions (Li < Na < K < Rb < Cs) at concentrations approaching silica saturation. When these observations are compared with concrete expansion in this and other studies [6-12] it seems obvious, that the dissolution kinetics at low Si concentrations match significantly better with the observed expansion than at high Si concentrations.

The alkali-silicate solution has to precipitate as a solid to cause expansion; its tendency to precipitate depends on whether the solution is (over)saturated with respect to the solid or it is not. The saturation

index of an alkali-silicate gel depends strongly on the concentration of calcium [16-18]. When calcium diffuses from the pore solution into the aggregate supersaturation can be reached and ASR products form. The gelling time in presence of calcium is also dependent on the type of alkali-silicate solution. The gelation time decreases in the following order: Cs > Rb > Li > K > Na [19]. However, neither the order in dissolution kinetics nor the one in gelation time is the same as the order of concrete expansion. The most notable example in this regard is concrete C-Rb exhibiting the highest expansion in spite of a relatively slow dissolution and gelation time. Excluding Rb, the effect of the other alkalis on dissolution rate shows a relation to concrete expansion.

Here, additional aspects have to be considered. The first one is the availability of the alkalis in the concrete pore solution over time. In the case of $LiNO_3$ between 22-30 % of the added amount is not in solution any more after two days of hydration [10]. Afterwards, Li concentration decreases more than K concentration with Na staying at a constant level during the first eight weeks [10]. The rapid reduction of Li during the first two days clearly shows that the cement hydrates are an important sink for alkalis. Moreover, Li is preferentially bound in ASR products compared to Na and K [11]. Although, no such data are available for the other alkalis, the selective binding by cement hydrates is expected to decrease the concentration of the added alkalis in the pore solution and with it their effect on expansion.

A second aspect is transport. The formation of ASR products ingresses from the surface of the aggregate to its interior filling pre-existing porosity. Alkalis, hydroxide, calcium and silicon are consumed by the precipitation of ASR products. In order to sustain the reaction, alkalis, hydroxide, calcium have to diffuse through already precipitated ASR products to reach the interior of the aggregate. The diffusion kinetics are likely dependent on the porosity and pore connectivity of the precipitated ASR products. The different added alkalis may have an effect on these diffusion characteristics. If this applies, ASR products containing Li may slow down ion diffusion more than for example ASR product containing Rb. However, this suggestion is purely hypothetical.

4.2 Composition of reaction products

The variations in the composition of the ASR products in the different concrete mixtures are in a similar range and show overlap. There are still differences that stand out, though. ASR products in concrete C-Li display the lowest average Ca/Si-ratio and show many points with a very low Ca/Si-ratio. This has already been reported in [10,20]. Synthesized Li-containing ASR products contain less Q_3-sites (SiO_2-tetraedra with three bridging oxygen forming a layer-structure) and seem to be denser than equivalent products containing Na and K [10]. This may translate a reduced diffusivity of the products leading to a protective layer on reactive minerals resulting in less dissolution. However, the dose used in concrete C-Li is relatively low which limits the suppressive effect of ASR from the addition of $LiNO_3$.

On the other end of the scale in regard to the Ca/Si-ratio is concrete C-K displaying both the highest mean values and the highest individual values. These values and the ones in concrete C-Rb and C-Cs match the ones present in ASR products formed in concrete structures [21-25], while the values of concrete C-Li and C-Na are relatively low. The Ca/Si-ratio may reflect the capability of the specific products to take up Ca or may be related to the advance of ASR. ASR products in a concrete with a more advanced ASR can be expected to display a higher Ca-Si-ratio compared to the situation in a less advanced reaction [13]. However, based on the identical age of the concrete and the achieved expansion after 8 weeks this seems not to be the case. Therefore, a more likely reason for the observed differences in the Ca/Si-ratio could be the radius of the hydrated alkalis. The radii of hydrated K, Rb and Cs ions are nearly identical, while the ones of Na and especially Li are larger approaching the one of Ca [26]. Consequently, Na and even more so Li could function in a similar way like Ca in the structure of the ASR products and as such limiting Ca incorporation.

The M/Si-ratio of the ASR products do not show a relation to expansion. It has to be noted that the M/Si-ratio cannot be determined correctly in concrete C-Li, because Li is not detectable with conventional EDS detectors. However, its presence in ASR products of Li-doped concrete has been confirmed by time-of-flight secondary ion mass spectrometry [10,11].

The Na/K-ratio of the ASR products reveals an interesting characteristic. While the addition of $NaNO_3$ clearly leads to an increased Na/K-ratio of 0.59, the KNO_3 addition does not result in significantly lower value with 0.25 compared to concrete C-Li, C-Rb and C-Cs. This is an effect of the cement composition. The Na/K ratio of the cement is 0.25. With the addition of $NaNO_3$, the Na/K-ratio of the concrete's alkali content is changed to 0.73 and in the case of the KNO_3 addition to 0.17. Consequently, the larger change in the Na/K-ratio of concrete C-Na is not an effect of preferential binding. The larger Na/K-ratio of the

ASR products in concrete C-Rb and C-Cs could indicate that Rb and Cs may replace some K. These three alkali have nearly identical radii in the hydrated state [26] making a certain replaceability feasible. There is no indication in the composition of the ASR products, why there is a correlation between expansion and atomic number of the alkalis (with the exclusion of Cs).

5. CONCLUSIONS

Concrete was doped with Li, Na, K, Rb and Cs in the form of nitrate. Its expansion was measured with the CPT at 60 °C and the composition of the ASR products formed in aggregates was determined by SEM-EDS after a reaction time of 8 weeks. Additionally, the impact of the different alkalis on SiO_2 dissolution kinetics was studied. Based on the results the following conclusions can be drawn:

- The different alkalis have an effect on SiO_2 dissolution kinetics. However, these differences are relatively small and do not agree with the differences in concrete expansion.
- Concrete expansion may not only depend on SiO_2 dissolution kinetics but as well on other factors like gelation time in the presence of Ca or differences in the density and diffusivity of the formed ASR products affecting ion transport to the ingressing reaction front.
- ASR products in concrete C-Li and C-Na contain less Ca than in the other concrete. This is possibly caused by larger ion radii of these alkalis, which could limit Ca uptake.
- The relatively low K content of the ASR products in concrete C-Rb and C-Cs indicates that these two alkalis can substitute part of K with a very similar hydrated ion radius.
- Rb and Cs addition increase the backscattering contrast of the ASR products making it possible to follow the sequence of reaction without applying EDS analysis. The formation of ASR products starts close to the surface of the aggregates and ingresses as a front towards the interior of the aggregates leading to the eventual cracking of the aggregate.

The data base should be broadened with concrete expansion obtained in the CPT at 38 °C. At this temperature SiO_2 dissolution is decreased and the effect of the different alkalis on expansion may be confirmed or may have to be re-evaluated.

6. ACKNOWLEDGEMENTS

The author would like to thank Barbara Lothenbach for reviewing the manuscript.

7. REFERENCES

[1] AFNOR XP 18-594 (2004) Méthodes d'essai de reactivité aux alcalis, Association Française de Normalisation, Paris.

[2] AFNOR P18-454 (2004) Réactivité d'une formule de béton vis-à-vis de l'alcali-réaction (essaie de performance), Association Française de Normalisation, Paris.

[3] C1260 - 14 (2014) Standard Test Method for Potential Alkali Reactivity of Aggregates (Mortar-Bar Method)

[4] C1293-18a (2018) Standard Test Method for Determination of Length Change of Concrete Due to Alkali-Silica Reaction.

[5] SN 505 262/1 (2019) Betonbau - Ergänzende Festlegungen. Schweizer Ingenieur- und Architektenverein, Zürich.

[6] Diamond S (1999) Unique response of $LiNO_3$ as an alkali silica reaction-preventive admixture. Cem Concr Res 29:1271-1275. https://doi.org/10.1016/S0008-8846(99)00115-5

[7] Fournier B, Stokes DB, Ferro A (2003) Comparative field and laboratory investigations on the use of supplementary cementing materials and lithium-based admixtures to control expansion due to alkali–silica reaction in concrete, 6th International CANMET/ACI Conference on Durability of Concrete, Thessaloniki, Greece, Supplementary Papers, pp. 823-851.

[8] Collins CL, Ideker JH, Willis GS, Kurtis KE (2004) Examination of the effects of LiOH, LiCl, and $LiNO_3$ on alkali–silica reaction. Cem Conc Res 34:1403-14015. https://doi.org/10.1016/j.cemconres.2004.01.011

[9] Tremblay C, Bérubé MA, Fournier B, Thomas MD, Folliard KJ (2007) Effectiveness of lithium-based products in concrete made with Canadian natural aggregates susceptible to alkali-silica reactivity. ACI Mater J 104:195-205.

[10] Leemann A, Lörtscher L, Bernard L, Le Saout G, Lothenbach B, Espinosa-Marzal RM (2014) Mitigation of ASR by the use of LiNO3 - characterization of the reaction products. Cem Concr Res 59:73-86. https://doi.org/10.1016/j.cemconres.2014.02.003

[11] Bernard L, Leemann A (2015) Assessing the potential of ToF-SIMS as a complementary approach to investigate cement-based materials - Applications related to alkali–silica reaction. Cem Concr Res 68:156-165. https://doi.org/10.1016/j.cemconres.2014.11.008

[12] Guo S, Dai Q, Si R. (2019) Effect of calcium and lithium on alkali-silica reaction kinetics and phase development. Cem Concr Res 115:220-229. https://doi.org/10.1016/j.cemconres.2018.10.007

[13] Leemann A, Münch B (2019) The addition of caesium to concrete with alkali-silica reaction: Implications on product identification and recognition of the reaction sequence. Cem Concr Res 120:27-35. https://doi.org/10.1016/j.cemconres.2019.03.016

[14] Leemann, A. (2017). Raman microscopy of alkali-silica reaction (ASR) products formed in concrete. Cem Concr Res 102:41-47. https://doi.org/10.1016/j.cemconres.2017.08.014

[15] Wijnen PWJG, Beelen TPM, De Haan JW, Rummens CPJ, Van de Ven, LJM, Van Santen RA (1989) Silica gel dissolution in aqueous alkali metal hydroxides studied by ^{29}Si NMR. J Non-Cryst Sol 109(1):85-94. https://doi.org/10.1016/0022-3093(89)90446-8

[16] Leemann A, Le Saout G, Winnefeld F, Rentsch D, Lothenbach B (2011) Alkali–silica reaction: the influence of calcium on silica dissolution and the formation of reaction products. J Am Ceram Soc 94(4):1243-1249. https://doi.org/10.1111/j.1551-2916.2010.04202.x

[17] Kim T, Olek J, Jeong H (2015) Alkali–silica reaction: kinetics of chemistry of pore solution and calcium hydroxide content in cementitious system. Cem Concr Res 71:36-45. https://doi.org/10.1016/j.cemconres.2015.01.017

[18] Shi Z, Lothenbach B (2019) The role of calcium on the formation of alkali-silica reaction products. Cem Concr Res 126:105898. https://doi.org/10.1016/j.cemconres.2019.105898

[19] Gaboriaud F, Nonat A, Chaumont D, Craievich A (1999) Aggregation and Gel Formation in Basic Silico-Calco-Alkaline Solutions Studied: A SAXS, SANS, and ELS Study. J Phys Chem B 103(28):5775-5781. https://doi.org/10.1021/jp990151s

[20] Kawamura M, Fuwa H (2003) Effects of lithium salts on ASR gel composition and expansion of mortars, Cem. Concr. Res. 33:913-919. https://doi.org/10.1016/S0008-8846(02)01092-X

[21] Thaulow N, Jakobsen UH, Clark B (1996) Composition of alkali silica gel and ettringite in concrete railroad ties: SEM-EDX and X-ray diffraction analyses. Cem Concr Res 26(2):309-318. https://doi.org/10.1016/0008-8846(95)00219-7

[22] Fernandes I (2009) Composition of alkali-silica reaction products at different locations within concrete structures. Mater Charact 60(7): 655-668. https://doi.org/10.1016/j.matchar.2009.01.011

[23] Katayama T, Drimalas T, Ideker JH, Fournier B (2012) ASR gels and their crystalline phases in concrete - universal products in alkali-silica, alkali-silicate and alkali-carbonate reactions. In Proceedings of the 14th International Conference on Alkali Aggregate Reactions (ICAAR), Austin, Texas, pp. 20-25.

[24] Leemann A, Lura P (2013) E-modulus of the alkali–silica-reaction product determined by micro-indentation. Constr Build Mater 44:221-227. https://doi.org/10.1016/j.conbuildmat.2013.03.018

[25] Leemann A, Merz C (2013) An attempt to validate the ultra-accelerated microbar and the concrete performance test with the degree of AAR-induced damage observed in concrete structures. Cem Concr Res 49:29-37. https://doi.org/10.1016/j.cemconres.2013.03.014

[26] Railsback, L. B. (2006). Some fundamentals of mineralogy and geochemistry. On-line book, quoted from: www.gly.uga.edu/railsback.